Bioresource Technology 136 (2013) 117–125

Contents lists available at SciVerse ScienceDirect

Bioresource Technology

journal homepage: www.elsevier.com/locate/biortech

Thermocatalytic treatment of biomass tar model compounds via radio frequency

Samsudin Anis [a,c], Z.A. Zainal [a,*], M.Z.A. Bakar [b]

[a] School of Mechanical Engineering, Universiti Sains Malaysia, Engineering Campus, 14300 Nibong Tebal, Penang, Malaysia
[b] School of Chemical Engineering, Universiti Sains Malaysia, Engineering Campus, 14300 Nibong Tebal, Penang, Malaysia
[c] Department of Mechanical Engineering, Universitas Negeri Semarang, Kampus Sekaran, Gunungpati, 50229 Semarang, Indonesia

HIGHLIGHTS

- A new effective tar thermocatalytic treatment using radio frequency energy is proposed.
- The reactor temperature of 1200 °C can be reached quickly at 700 W.
- RF non-thermal effect contributes for generating radical reaction for tar removal.
- Y-zeolite has better catalytic activity than dolomite, even at temperature of 550 °C.

ARTICLE INFO

Article history:
Received 5 December 2012
Received in revised form 13 February 2013
Accepted 17 February 2013
Available online 24 February 2013

Keywords:
Radio frequency
Thermocatalytic treatment
Tar
Toluene
Naphthalene

ABSTRACT

A new effective RF tar thermocatalytic treatment process with low energy intensive has been proposed to remove tar from biomass gasification. Toluene and naphthalene as biomass tar model compounds were removed via both thermal and catalytic treatment over a wide temperature range from 850 °C to 1200 °C and 450 °C to 900 °C, respectively at residence time of 0–0.7 s. Thermal characteristics of the new technique are also described in this paper. This study clearly clarified that toluene was much easier to be removed than naphthalene. Soot was found as the final product of thermal treatment of the tar model and completely removed during catalytic treatment. Radical reactions generated by RF non-thermal effect improve the tar removal. The study showed that Y-zeolite has better catalytic activity compared to dolomite on toluene and naphthalene removal due to its acidic nature and large surface area, even at lower reaction temperature of about 550 °C.

© 2013 Elsevier Ltd. All rights reserved.

1. Introduction

Tar as one of the undesirable byproducts produced during biomass gasification processes is a major problem that has not been completely solved yet. Due to its high concentration, upon condensation tar can block downstream pipelines and foul engines and turbines. Typically tar contents of producer gas produced from downdraft, updraft and fluidized bed gasifiers are about 1 g Nm^{-3}, 100 g Nm^{-3} and 10 g Nm^{-3}, respectively (Milne et al., 1998). Meanwhile tar content tolerances of downstream applications are very strict where tar contents up to 100 mg Nm^{-3} and less than 5 mg Nm^{-3} are allowed for internal combustion engines and gas turbines, respectively (Milne et al., 1998).

The present tar reduction methods comprise of gasifier design, mechanical, thermal and catalytic (thermocatalytic) treatment. Gasifier design has not yet resulted in satisfactorily solution because of the limits in feedstock flexibility, decrease in cold gas efficiency, and complex gasifier constructions (Bergman et al., 2003). It has not significantly reduced the tar content. The amount of tar produced during steam gasification in a fast internally circulating fluidized-bed gasifier (FICFB) of about 1 g Nm^{-3} has been obtained (Hofbauer et al., 1997). Mechanical treatments can potentially reduce energy conversion efficiency, clogging of apparatus, and uneconomic sludge treatment (Anis and Zainal, 2011; Lee et al., 2008). Meanwhile thermocatalytic treatments especially in secondary reactor are rather promising because of the complete tar reduction instead of creating a waste stream (Anis and Zainal, 2011).

Many literatures regarding tar thermal treatment have been performed, mostly done below 1100 °C with relatively low tar removal efficiency. Only few works were concerned at temperature higher than 1100 °C (Jess, 1996; Zhang et al., 2010) that provides high tar removal efficiency. Previous study showed that the temperature of 1200 °C and residence time less than 10 s are needed to achieve high tar removal efficiency (Jess, 1996). Certainly, the

* Corresponding author. Tel.: +60 4 5937788; fax: +60 4 5941025.
E-mail address: mezainal@eng.usm.my (Z.A. Zainal).

0960-8524/$ - see front matter © 2013 Elsevier Ltd. All rights reserved.
http://dx.doi.org/10.1016/j.biortech.2013.02.049

high reaction temperatures require high energy that impacts to overall energy efficiency make it uneconomically feasible for practical application. The catalytic treatment of tar using various catalysts also has been reported in many literatures. The most widely used catalysts are basic and acid catalysts such as dolomite, olivine, zeolite and silica–alumina. Calcined dolomite is a very well-known catalyst for tar removal that is inexpensive and prevents agglomeration (Corella et al., 2004). Its activity becomes important at temperature above 800 °C. While zeolite is a commercial catalytic cracking (FCC) catalyst and has been proven as an active tar removal catalyst, improves the gaseous quality with relatively low-price. However, the fine particle size of zeolites makes it unsuitable for high flow rate catalytic tar decomposition (Corella et al., 2004). On the other hand, very limited research has been performed regarding application of zeolites especially Y-zeolite for tar model compounds removal such as benzene (Radwan et al., 2000), 1-methylnaphthalene (Dou et al., 2003) and naphthalene under steam reforming at relatively high temperature of 750 °C (Buchireddy et al., 2010).

In general, although thermocatalytic treatment of tar is very effective for tar removal at high temperatures, but the overall process is expensive and high energy demand. This is because majority of thermocatalytic treatment of tar research is directed at conventional heating mechanism using an external high electrical source where heat transfer occurs from the surface to the core of the material. Another drawback is the lack of rapid heating, heat transfer resistance, heat losses to surrounding and damage to reactor walls due to continuous electrical heating (Salema and Ani, 2011). Accordingly, there is a need for a more economical method.

In order to support the development and operation of a commercial tar thermocatalytic treatment method, it is desirable to have a simple and rapid test technique that is economically feasible. For this reason, the use of radio frequency (RF) energy in this research is believed to be an alternative method to solve the limitations of conventional heating method. In this method which commonly utilizes microwave, the transfer of energy into the material occurs instantaneously through molecular interaction with the electromagnetic field (Thostenson and Chou, 1999). The volumetric heating of materials using RF can result in significant energy savings, reduce process time, increase process yield and environmental compatibility (Bykov et al., 2001; Jones et al., 2002). The additional advantages of RF heating in the field of waste treatment including off gas treatment are: (1) rapid heating, (2) high temperature capabilities, (3) selective heating, (4) enhanced chemical reactivity, (5) rapid and flexible process that can also be made remote, (6) ease of control, (7) process equipment availability, compactness, cost, maintainability, (8) portability of equipment and process, (9) cleaner energy source compared to some more conventional systems, and (10) overall cost effectiveness/savings (Wicks et al., 1998). A more comprehensive review on the unique characteristics of RF heating and its application for biomass pyrolysis has been reported (Yin, 2012).

Therefore, in the present research, thermal characteristics of a modified RF system and its application for thermocatalytic treatment of tarry materials are developed. This research has high prospect in providing basic knowledge into the fundamentals of tar thermocatalytic treatment via RF irradiation that is cost effective, clean energy source, simplicity and potential for process scale up. In addition, it is expected that the high electromagnetic irradiation intensity not only provide rapid heating and high temperature but also increase radical reactions that are responsible for tar removal.

With the aim to obtain optimal conditions and achievable technical performance for the proposed new RF tar thermocatalytic treatment process in term of temperature evolution within the reactor, various parameters including susceptor material particle size, bed height, gas flow rate and power were tested. Moreover, in order to remove the tar effectively during thermocatalytic treatment, two catalysts (dolomite and Y-zeolite), various temperatures and residence times were also investigated using toluene and naphthalene as tar model compounds.

2. Methods

2.1. Materials

Toluene and naphthalene (commercial grade) were used as tar model compounds and are good representative for biomass tar (El-Rub, 2008; Simell et al., 1997). Toluene (C_7H_8) is a light aromatic hydrocarbon (LAH) with single ring compound which is a class 3 tar, whilst naphthalene ($C_{10}H_8$) is a light poly-aromatic hydrocarbon (LPAH) with two rings compound which is a class 4 tar. Biomass tar produced by fluidized beds and downdraft gasifiers typically is classified as class 3 and 4 tar (Milne et al., 1998). Purified nitrogen (99.999%) was used as a carrier gas to purge the evaporated tar model and to keep the atmosphere inert. Two catalytic materials: dolomite and Y-zeolite were used to remove tar compounds in this study. Dolomite is a naturally occurring mineral whilst Y-zeolite is a commercial catalyst. The properties of both catalysts are presented in Table 1. Four particle sizes of silicon carbide (SiC): F10, F12, F14 and F16 were used as susceptor materials. The physical properties of SiC in accordance with FEPA-Standard 42-GB-1984 R 1993 and 42-GB-1986 R 1993 are shown in Table 2. SiC is known as a good RF susceptor material that can absorb and convert the RF energy into heat by conduction due to the high dielectric loss and a relaxation time according to the changes of RF dipole directions (Thostenson and Chou, 1999). Besides, SiC also does not have any catalytic effect in the decomposition of tar (Simell et al., 1997).

2.2. Experimental apparatus

The experimental apparatus consists of a modified RF oven, reactor, tar generator, mixing chamber, tar collector, and measuring systems. A schematic diagram of the experimental apparatus is presented in Fig. 1(a).

A modified domestic RF oven (Panasonic, NN-SM330 M) with a maximum output power of 700 W and frequency of 2450 MHz, equipped with variable power and time was used in the experiments. A reactor (25.4 mm i.d. and 160 mm length) vertically installed in the RF chamber and constructed of a ceramic material (alumina) is able to withstand temperature up to 1600 °C. An insulating material (asbestos blanket) covers the reactor to prevent excessive temperature inside the RF chamber from damaging the RF oven. A K-type thermocouple was used to monitor the temperature inside the RF chamber. Both the reactor and insulating

Table 1
Properties of catalysts.

Y-zeolite	
SiO_2/Al_2O_3	30
Na_2O (wt.%)	0.03%
Unit cell size (Å)	24.28
Surface area (m^2/g)	780
Pore size (Å)	7.4
Calcination	550 °C for 2 h
Dolomite	
Composition (wt.%)	34.69% CaO, 15.06% MgO, 2.34% SiO_2, 1.07% Al_2O_3, 0.61% Fe_2O_3
Particle size (μm)	600
Calcination	900 °C for 1 h

Table 2
Bulk density and grain size distribution of the SiC particles.

Grit designation (FEPA standard)	Bulk density (g/cm^3)	Grain size distribution (μm)	(%)	Mean (μm)
F10	1.48	3350	0	2085
		2360	19	
		2000	52	
		1700	78	
		1400	81	
		<1400	0	
F12	1.53	2800	0	1765
		2000	8	
		1700	48	
		1400	87	
		1180	91	
		<1180	1	
F14	1.55	2360	0	1470
		1700	11	
		1400	64	
		1180	85	
		1000	89	
		<1000	0	
F16	1.56	2000	0	1230
		1400	17	
		1180	48	
		1000	78	
		850	83	
		<850	0	

materials are transparent to RF irradiation. The reactor contains susceptor material (SiC) and a moveable temperature detector (K-type thermocouple) at the center of the reactor. The susceptor material was supported on a stainless steel grate. The system was designed such that the susceptor material inside the reactor can be easily handled.

Tar generator (100 mm i.d., 120 mm height) and mixing chamber (50 mm i.d., 100 mm height) were made of stainless steel. Tar generator was designed to evaporate toluene and naphthalene whereas mixing chamber was used to ensure homogeneity of the evaporated tar and carrier gas mixture. The tar generator was heated by a gas stove for rapid tar evaporation at temperature of 250 °C. The mixing chamber was heated by an induction heater to ensure the temperature of the insulated piping system was above the tar models dew point. An analytical micro balance model TB-413 with accuracy of 0.001 g was used to determine the mass of toluene or naphthalene evaporated before thermocatalytic treatment and mass of condensed product after process.

2.3. Thermal heating experiment

The thermal effect of various RF powers (135–700 W), gas flow rates (5–15 LPM), bed heights (40–120 mm) and particle sizes of susceptor material (F10–F16) on temperature profile inside the reactor were investigated. The purified nitrogen was passed through the system from the bottom of the reactor and regulated using a flow meter and a valve.

During the experiment, temperatures within the reactor and RF chamber were recorded every 5 s for 20 min of irradiation using a 12 channel Digi-Sense temperature data logger model 69292-30. Temperature was measured using a 3 mm o.d. K-type stainless steel sheathed thermocouple that satisfies measurement of temperature in electromagnetic field. Grounding of the metallic sheath to the chamber is required to avoid arcing. After the designated irradiation time, the RF oven was automatically switched off and the gas turned off. Then, the system was allowed to cool to ambient

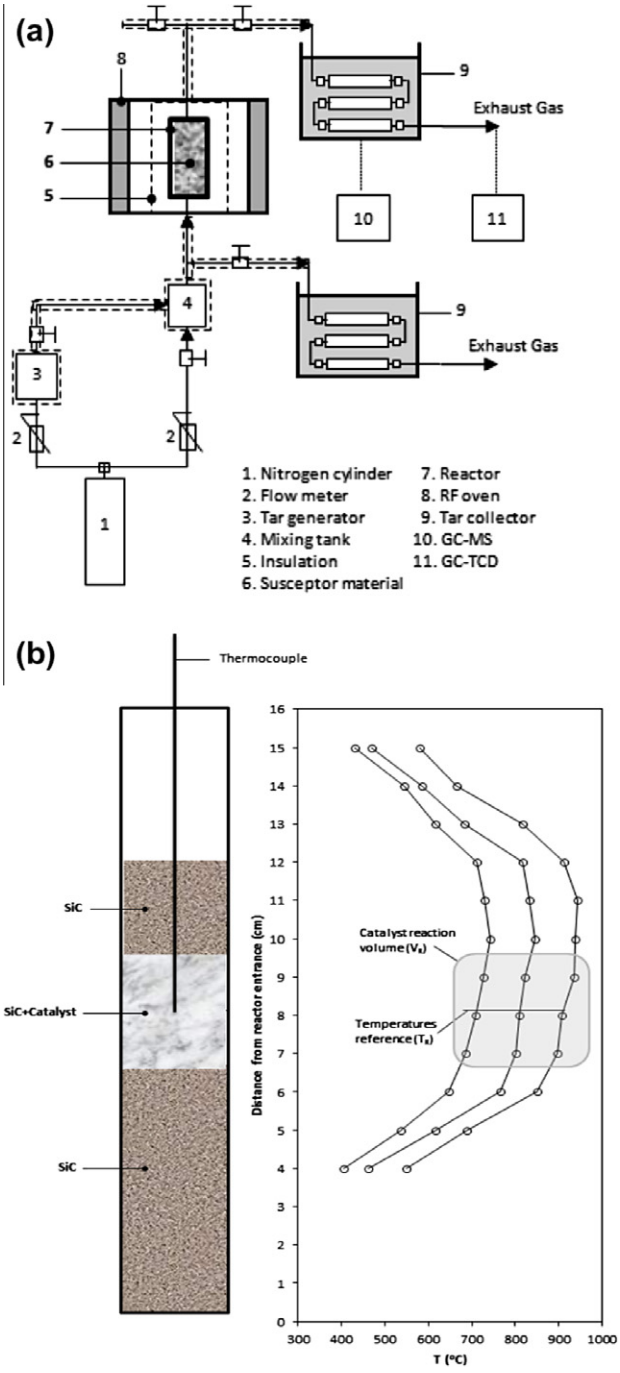

Fig. 1. A schematic diagram of the experimental apparatus (a); temperature profiles and some reference temperatures for catalytic treatment of tar models (b).

temperature. This procedure was repeated for each set of reaction conditions investigated.

2.4. Thermocatalytic treatment of tar model compounds

Experimental activities were focused to remove the tar model compounds via both thermal and catalytic treatment process. For each experiment, the tar model compound was evaporated in the tar generator and carried with purified nitrogen gas into the RF tar treatment reactor. During the experiment, the purified nitrogen gas was continuously supplied at a particular flow rate to give the desired residence time as well as to maintain inert atmosphere to

prevent oxidation of the products. Part of the purified nitrogen flowed through the tar generator containing toluene or naphthalene and then mixed with the main nitrogen in the mixing chamber to obtain the desired initial concentration of the evaporated tar model.

In case of thermal treatment, the initial concentration of the evaporated tar model was fixed at 100 g Nm^{-3}, whereas the residence time in the susceptor bed material with respect to the empty bed volume at standard temperature and pressure (s.t.p.) condition was varied from 0 to 0.7 s. Temperature for toluene removal in this work was conducted between 850 °C and 1050 °C, whereas for naphthalene removal process was operated between 900 °C and 1200 °C based on Evans and Milne (1997). For catalytic treatment, the bed was arranged into three layers: SiC, catalyst + SiC mixture, and SiC particles at top layer as shown in Fig. 1(b). In each experimental run 10 g of dolomite or 6 g of Y-zeolite was mixed with 25 g of SiC for preparing the bed with a height of 30 mm. The initial concentration of the evaporated tar model and the residence time within the catalyst bed were fixed at 50 g Nm^{-3} and 0.24 s (s.t.p.), respectively. The catalyst bed temperature for toluene or naphthalene removal was conducted at a lower temperature between 450 °C and 900 °C due to catalyst thermal stability (Gates, 1992) and to avoid the thermal treatment effect. Temperature profiles and some reference temperatures measured in the reactor for catalytic treatment of tar model compounds are given in Fig. 1(b).

Before and after leaving the reactor, the gas flow was led into a tar collector and a cotton filter to condense the tar as well as to capture the soot produced during thermocatalytic treatment process. The tar collector consists of three glass bulbs with volume of 250 mL each. They were immersed in a mixture of ice and salt bath with temperature of about −22 °C which is enough to condense the light and heavy tar compounds (Bergman et al., 2003).

The clean gas product was collected using gas sampling bag and then analyzed in a Gas Chromatography–Thermal Conductivity Detector (GC–TCD) to quantify the amount of H_2 and C_1–C_2 hydrocarbons. The condensed products in this work refer to the condensed residual tar model compounds and the higher hydrocarbons produced during polymerization and condensation reactions whereas soot refers to the solid carbonaceous product. Total condensed product and soot remained in the tar collector, cotton filter and connecting tube were determined via weight difference of the equipments before and after the experiments. The equipments can be easily dismantled in order to weigh them individually and reconnect back for further experiments. After that, the condensable products were carefully washed and collected by using acetone. The solutions were then filtered through preweighed qualitative filter paper (Whatman, 90 mm diameter) into a preweighed flask to separate the solid particles (soot). The solvent was evaporated and dried at 40 °C for 1 h in a drying oven. The amount of soot remaining in the equipments and filter paper was weighed at the end of the experiments to investigate the yield. Whilst, the yield of soot deposited on catalysts was determined by means of combustion method using a Thermogravimetric Analyzer (TGA). Finally, tar samples were analyzed by Gas Chromatography–Mass Spectrometry (GC–MS) analyzer with NIST MS 2.0 software. The mass spectrum was acquired using a quadrupole instrument with an electron voltage of 70 eV. The GC column was a DB-5MS column, 30 m long, 0.25 mm diameter, with a film thickness of 0.25 μm, and helium flow rate of 1 mL min^{-1}. The column oven temperature was programmed from 65 °C (held for 2 min) to 300 °C at 8 °C min^{-1} and then held for 10 min. Each sample volume is 1 μL. Three samples were taken to obtain the average. In general more than 95% mass balance in thermocatalytic treatment of tar models was obtained.

3. Results and discussion

3.1. Temperature profiles

3.1.1. Effect of susceptor material particle size

A series of studies were performed in order to determine the effect of particle sizes of SiC as susceptor material on the performance of RF thermal heating. Fig. 2(a) shows the temperature evolutions of four particle sizes, 2.085 mm (F10), 1.765 mm (F12), 1.470 mm (F14), and 1.230 mm (F16), at RF power of 700 W, gas flow rate of 10 LPM, and height of susceptor material within the reactor of 120 mm. It can be seen that smaller particle size produces higher reactor temperature and heating rate. The temperatures of each particle sizes at irradiation time of 20 min reach 1206 °C, 1196 °C, 1179 °C, and 1168 °C for F16, F14, F12, and F10, respectively. The heating rates were in the same order i.e. 54.82 °C min^{-1}, 54.54 °C min^{-1}, 54.06 °C min^{-1}, and 52.56 °C min^{-1}, respectively. It was also shown that at the first 5 min of irradiation, the reactor temperature of the larger sample size increased slowly and become significant at further irradiation time. Based on the penetration depth of RF power the incident power is reduced to $1/e$ ($e = 2.718$) of its initial value at the surface of particles. When RF energy transmits through an absorber material, a part of the RF energy is converted into heat and the remaining power decreases with distance from the surface of material. Lambert's law describes clearly that RF power reduction is a function of distance (z) as shown in Eq. (1) (Tang et al., 2002):

$$P(z) = P_o e^{-2\alpha z} \quad (1)$$

where P_o is incident RF power at the surface, $P(z)$ is RF power at distance z in the direction of RF propagation within the absorber material, and α is the attenuation constant.

From Eq. (1), the RF power decreases exponentially with the depth of absorber material. This means that absorber material with smaller size reaches faster and higher temperature. Moreover, the RF power requirement can also be reduced with smaller particle size (Huang et al., 2008). Nevertheless, in this study, both the reactor temperature and heating rate were only slightly different for all particle sizes tested during 20 min of irradiation. The differences of the reactor temperature as well as the heating rate of each sample were less than 5%. For this particle size range, the RF energy is enough to penetrate into the particles and might only focus on one hotspot.

3.1.2. Effect of bed height

Effect of bed height on the performance of RF thermal heating was studied by varying the height of susceptor material at 40 mm, 80 mm, and 120 mm under RF power of 700 W, gas flow rate of 10 LPM, and susceptor material particle size of F10. Fig. 2(b) describes the increase of reactor temperature with the increase of bed height. The system with lower bed height have lower absorbed RF power therefore the reactor temperature is also lower than that of the system with higher bed height. It can be seen that the reactor temperature increased sharply for the first 2 min of irradiation for both 40 mm and 80 mm. Beyond 2 min, the reactor temperature remained constant for bed height of 40 mm but increased slowly for 80 mm. While for bed height of 120 mm, the reactor temperature increased significantly during 20 min of irradiation tested. As shown in Eq. (2) (Sutton, 1989), the absorbed RF power increases as the volume of the susceptor material increases, which is concurrent with this study (Salema and Ani, 2011):

$$P_{abs} = 2\pi f \varepsilon_o \varepsilon'' E^2 V \quad (2)$$

where P_{abs} is the absorbed RF power (W), f is frequency (Hz), ε_o is the permittivity of free space (8.85×10^{-12} F m^{-1}), ε'' is dielectric loss factor, E is electric field (V m^{-1}), and V is volume of material (m^3).

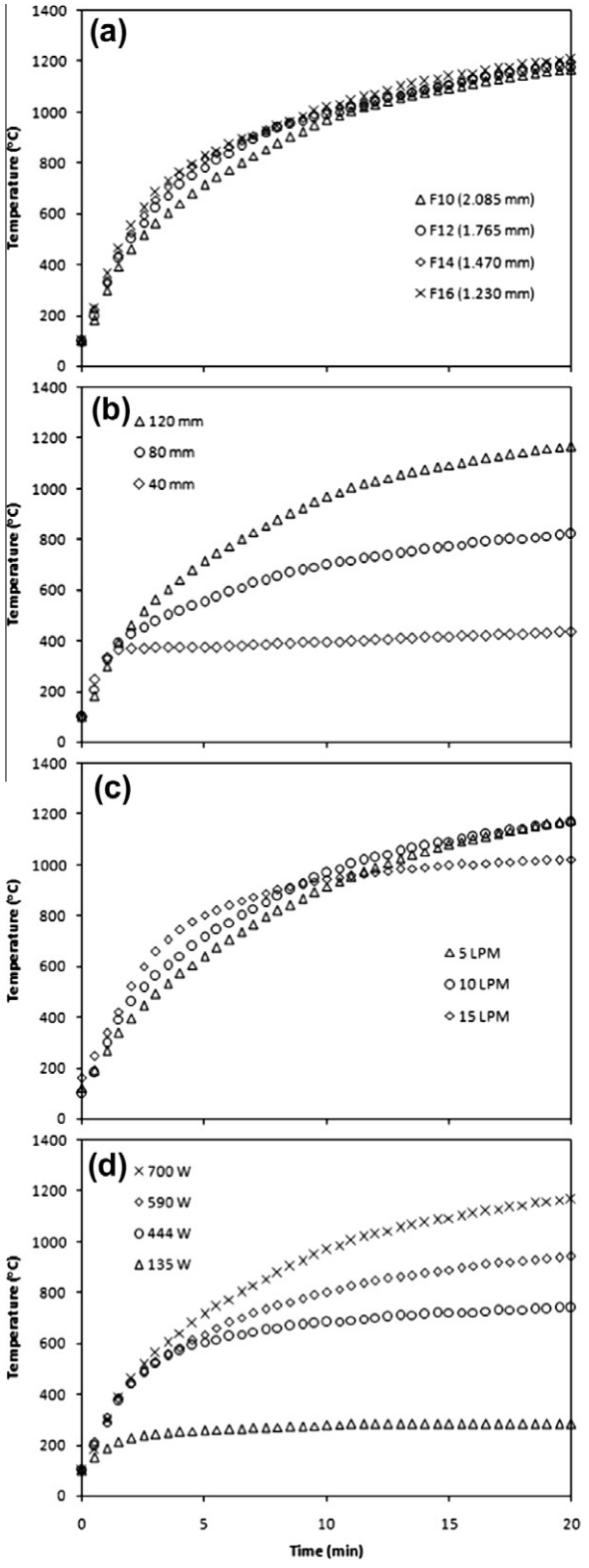

Fig. 2. Temperature profiles within the reactor: (a) effect of susceptor material particle size; (b) effect of bed height; (c) effect of gas flow rate; (d) effect of RF power.

3.1.3. Effect of gas flow rate

Gas flow rate was varied at 5 LPM, 10 LPM and 15 LPM to study its effect on thermal heating in the RF system under RF power of 700 W, bed height of 120 mm, and susceptor material particle size of F10. The result of thermal heating indicated by the reactor temperature during 20 min of irradiation is shown in Fig. 2(c). Appropriate gas flow rates need to be selected for optimal performance of the system. It was found that the gas flow rate of 10 LPM has the highest heating rate compared to the other two flow rates. The figure also shows that the reactor temperature increased significantly for the first 5 min of irradiation and then increased gradually for gas flow rate of 5 LPM and 10 LPM. This is because the rate of heat convection to heat up all the particles of susceptor material was lower, therefore needing longer time to obtain uniform temperature within the reactor. Conversely at 15 LPM gas flow rate, the reactor temperature increased more significantly for the first 5 min of irradiation, beyond which, the reactor temperature increased slowly and finally constant. The heat generated by the absorbed RF power in the susceptor material can quickly be distributed to other particles along the reactor. Nevertheless, after optimum condition was reached, the high gas flow rate with lower temperature caused cooling effect or convective cooling at the material surface. The convective cooling in some circumstances may be described by Newton's law of cooling.

3.1.4. Effect of RF power

The temperature profiles within the reactor under different RF power are shown in Fig. 2(d). In this study, other parameters were kept constant i.e. bed height was 120 mm, gas flow rate was 10 LPM, and particle size of susceptor material was F10. As shown, the reactor temperature increases as the RF power increases. At RF powers of 135 W and 444 W, the temperatures increased significantly for the first 2 and 4 min of irradiation, respectively. Beyond these times, the temperatures became constant for RF power of 135 W but increased slowly for 444 W. At irradiation time of 20 min, the maximum temperatures were only 283 °C and 743 °C, respectively. More promising results were obtained at 590 W and 700 W where the temperatures increase significantly and reach 943 °C and 1168 °C, respectively at 20 min of irradiation. These cases show that the absorbed RF power into the material increases as the incident RF power increases, therefore temperature within the reactor will also increase. The results were in compliance with Eq. (2) as expressed before where the absorbed RF power is strongly affected by the electric field. In addition, the increase of the electric field will also result in more rapid heating inside the reactor so reduce the required heating time. In this study, the reactor temperature of 900 °C can be reached in 8 min irradiation for 700 W while 15 min was required with 590 W.

Heating rates at different time intervals are shown in Table 3. They were calculated from the slope of linear regression of temperatures every 5 min of irradiation interval. It was observed that for RF powers of 590 W and 700 W, the heating rates reduced gradually during 20 min of irradiation. In contrast, for lower RF powers (135 W and 444 W), a lower heating rates were observed. Generally, the highest heating rates were reached in the first 5 min of irradiation i.e. 25.99 °C min^{-1}, 98.80 °C min^{-1}, 98.83 °C min^{-1}, and 120.10 °C min^{-1} for 135 W, 444 W, 590 W, and 700 W, respectively. While, at irradiation intervals of 15–20 min, the heating rates were only 0.39 °C min^{-1}, 4.28 °C min^{-1}, 10.27 °C min^{-1}, and 15.51 °C min^{-1}, respectively. The similar behavior was also reported by Huang et al. (2010). The heating rate reduction is attributed to the penetration depth of RF power decreases when temperature of the material rises. The penetration depth of RF power (D_p) can be determined using the following equation (Clark and Sutton, 1996):

Table 3
Heating rates (°C min^{-1}) under different RF power.

RF power (W)	Time interval (min)			
	0–5	5–10	10–15	15–20
50	25.991	4.098	0.618	0.394
380	98.805	15.927	8.174	4.275
540	98.837	32.071	17.013	10.271
700	120.141	50.877	24.334	15.513

$$D_p = \frac{\lambda_0}{2\pi\sqrt{2\varepsilon'}}\left[\sqrt{1+\left(\frac{\varepsilon''}{\varepsilon'}\right)^2}-1\right]^{-1/2} \quad (3)$$

where λ_0 is free space wavelength of the RF radiation, ε' and ε'' are the relative values of the dielectric constant and loss factor, respectively.

As shown in Eq. (3), the penetration depth of RF power depends on the dielectric properties of the susceptor material. On the other hand, at a fixed frequency, the dielectric properties of both the relative values of the dielectric constant and loss factor depend mainly on temperature. In general, the behavior of these two properties of absorber materials would increase when temperature increases. For instance, SiC used in this study has a loss factor of 1.71 at room temperature at frequency of 2.45 GHz, while at 695 °C for the same frequency is 27.99 (Sutton, 1992). Therefore, the penetration depth of RF power into material changes during processing.

3.2. Thermal treatment of tar model compounds

Thermal treatment of toluene and naphthalene as a function of temperature at a constant residence time of 0.5 s is shown in Fig. 3. As shown, the reactivity of toluene was higher than that of naphthalene. This confirms the study of Jess (1996) that the order of reactivity was obtained as toluene ≫ naphthalene > benzene. In this study, toluene removal was studied at various temperatures of 850–1050 °C as given in Fig. 3(a). Organic soot as a treatment product appeared immediately at 850 °C. The yield of condensed product at temperature of 1000 °C reached 16% accompanied by black soot formation. Further increase of temperature increases soot formation and reduces the condensed product, in which at temperature of 1050 °C about 22% of soot and 9% of condensed product were found. The gas species also increase significantly as temperature increases. At the highest temperature tested, CH_4 formed as the major product. In another case, naphthalene seems thermally stable and hard to be removed at temperatures below 1100 °C where 77% of condensed product was obtained at temperature of 1050 °C as shown in Fig. 3(b). Study showed that naphthalene removal increases significantly with the increase of temperatures from 1100 °C to 1200 °C. At these conditions, although the formation of gaseous products increased considerably especially H_2, however soot appeared as the main product during thermal treatment of naphthalene. The lowest yield of condensed product of 9% and the highest yield of soot product of about 68% were obtained at 1200 °C. The main reactions during thermal treatment of tar models (C_xH_y) are shown below:

– Cracking reaction:

$$pC_xH_y \rightarrow qC_nH_m + rH_2; \quad n < x \text{ and } m < y \quad (4)$$

– Carbon formation:

$$C_xH_y \rightarrow xC + (y/2)H_2 \quad (5)$$

– Hydrogen–carbon reaction (methane formation):

$$pC + qH_2 \rightarrow rCH_4 \quad (6)$$

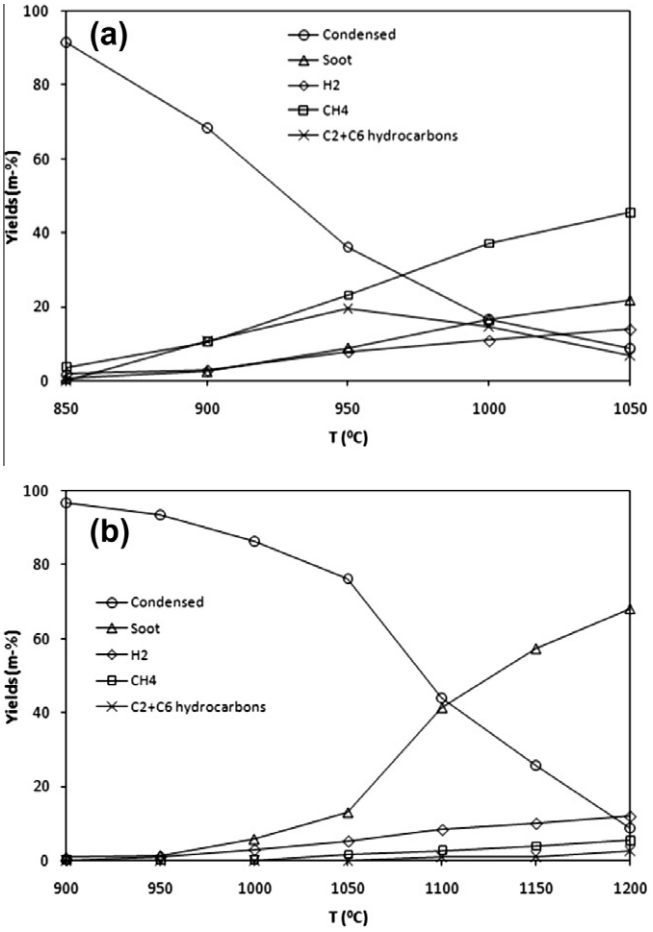

Fig. 3. Products yields during thermal treatment of tar models as a function of temperatures: (a) toluene and (b) naphthalene.

– Hydrocracking:

$$C_xH_y + pH_2 \rightarrow qCH_4 \quad (7)$$

Tar species and soot for three different temperatures during RF-assisted thermal treatment of toluene and naphthalene are depicted in Fig. 4. As shown, the yield of LPAH (2–3 rings compounds) and heavy PAH (HPAH, more than three rings compounds) for toluene removal are obviously different with that of naphthalene. In case of toluene removal, the hydrocarbon will grow to form PAHs and ultimately forming soot. From the results, the formation process of PAHs began at temperature of 850 °C while the formation of soot appeared at temperature of about 950 °C. The yield of LPAH reached a maximum as the increase of reaction temperature to 1000 °C as shown in Fig. 4(a). Further increase in temperature, the yield of LPAH decreased and the formation of HPAH took on more prominent role due to polymerization. The figure also showed that both LPAH and HPAH contribute in soot formation. Fig. 4(b) indicates that the yield of both LPAH and HPAH produced from naphthalene removal decreased with the increase of reaction temperature. This result is contradictory with soot formation which increases as the temperature increases. It means that at very high temperature naphthalene can be kinetically converted into soot. This is confirmed also by Jess (1996) that practically only soot was left at temperatures of higher than 1200 °C.

Based on the reaction temperature, the following two mechanisms are possible for thermal treatment of tar models (toluene and naphthalene) in pure N_2 stream used in this study: (1) at

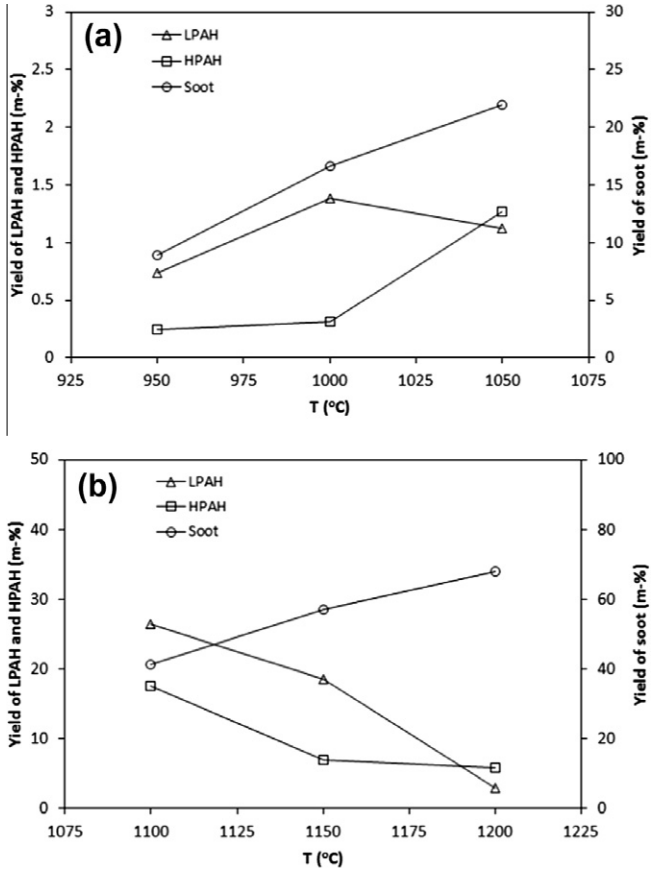

Fig. 4. Tar compounds contained in condensed products during thermal treatment of tar models as a function of temperatures: (a) toluene and (b) naphthalene.

relatively lower reaction temperature, the tar model is only converted into LAH and LPAH (1–3 rings compounds), hydrogen and hydrocarbon gases; and (2) at relatively higher reaction temperature, the tar model is converted into hydrogen, hydrocarbon gases, LAH, LPAH, HPAH and soot. From those two mechanisms given, toluene and naphthalene removal in this study comply the hydrogen abstraction carbon addition (HACA) method proposed by Frenklach and Wang (1994). This method has also been adopted in other studies to define the reaction scheme of thermal conversion of aromatic hydrocarbons and biomass gravimetric tar (Jess, 1996; Namioka et al., 2009).

Effect of gas residence time on thermal treatment of biomass tar model compounds is also studied. The experiments were conducted at residence time of 0–0.7 s and at a constant temperature of 950 °C for toluene and 1100 °C for naphthalene. The results showed that the removal efficiency of both toluene and naphthalene increased with the increase of gas residence time. Longer residence time favors thermal treatment of tar as reported in other studies (Fassinoua et al., 2009; Jess, 1996). Conversely, for shorter residence time the reaction rate limits the removal of toluene and naphthalene. It was observed that the removal efficiency of toluene reached only 38% at 0.2 s and about 75% at 0.7 s whereas for naphthalene the removal efficiency were obtained only 30% at 0.2 s and about 68% at 0.7 s.

Although toluene and naphthalene can be removed by thermal treatment, however the production of a lot of soot particularly from naphthalene becomes a new problem that must be solved. Several efforts have been demonstrated for reducing soot production (Boroson et al., 1989; Jess, 1996; Zhang et al., 2010). The first is the presence of H_2, O_2 or CO_2 that can kinetically inhibit soot formation by hydrogenation, partial combustion or dry gasification reaction, respectively. The second is the use of steam as a reforming agent that converts the soot into CO and CO_2 via either water gas shift reaction or carbon gasification reaction. The third is the use of catalysts where the soot is trapped on the catalyst surface and decomposes into valuable gases at lower temperature, and the fourth is the combination of these methods. Therefore, in order to remove tar as well as soot simultaneously, the third way was chosen and tested in this study. Details of experimental results are described in the following section.

3.3. Catalytic treatment of tar model compounds

Effect of catalysts (dolomite and Y-zeolite) on tar removal efficiency was tested at two different temperatures (650 °C and 700 °C) using toluene and naphthalene as tar model compounds. The results found that dolomite showed lower tar removal efficiency in comparison with Y-zeolite in all investigated condition. Toluene removal efficiency of about 30% and 82% were observed for dolomite and Y-zeolite, respectively at temperature of 650 °C and gas residence time of 0.24 s. As is the case in toluene removal, the activity of dolomite on naphthalene removal is also inferior to that of Y-zeolite. The naphthalene removal efficiencies of about 33% and 79% were obtained at temperature of 700 °C for dolomite and Y-zeolite, respectively. The difference in activity is mainly caused by the differences of physical and chemical properties of both catalysts as shown in Table 1.

Literatures showed that the average pore diameter of dolomite is commonly above 7 nm (Gusta et al., 2009) whilst Y-zeolite has a pore size of about 0.74 nm (see Table 1). On the other hand, molecular dimension of toluene and naphthalene are in the range of 0.49–0.73 nm (Gates, 1992). This indicated that the pore sizes of both catalysts allow toluene and naphthalene to diffuse into their pores. In most cases, the higher catalytic activity of Y-zeolite compared to dolomite is, however, due to its acidic nature that supports removal of toluene and naphthalene. Moreover, the high activity of Y-zeolite is also due to its higher surface area ($780\ m^2\ g^{-1}$) than dolomite. Similar behaviors to the activity of Y-zeolites toward other tar models conversion were obtained in conventional heating (Buchireddy et al., 2010; Dou et al., 2003).

The removal of toluene and naphthalene using dolomite as a catalyst at various tested temperatures are shown in Fig. 5. In this case, the removal of toluene and naphthalene were conducted in the temperature range of 650–850 °C and 700–900 °C, respectively, in order to minimize the effect of thermal treatment of the tar models as already been described previously. As shown, temperature plays an important role in the removal of the tar models. In general, the yield of gas products increases with increase in temperature, whereas condensed product and soot decreased. Fig. 5(a) indicates that almost a third of condensed product was removed from 650 °C to 850 °C during catalytic treatment of toluene using dolomite. This result corresponds to the yield of condensed product of about 70% and 24% at 650 °C and 850 °C, respectively. Meanwhile, the amount of condensed product provided from catalytic treatment of naphthalene can be reduced about twofold from 700 °C to 900 °C in which the yield of condensed product of about 67% and 33% were obtained at 700 °C and 900 °C, respectively as shown in Fig. 5(b). The comparison of toluene and naphthalene removal using dolomite is also pointed out in the figure. Under the same operating condition (700–850 °C), the reactivity of toluene is higher than that of naphthalene. The removal of toluene showed significant improvement at higher temperature in which H_2 and CH_4 appeared as the important products. According to previous studies, naphthalene is the most stable and difficult compound to be removed using dolomite as a catalyst (Devi et al., 2005). Soot upon dolomite surface was also observed under the experimental conditions. A small portion of dolomite turned black particularly at the bottom part and the remainder turned grey. This is due to

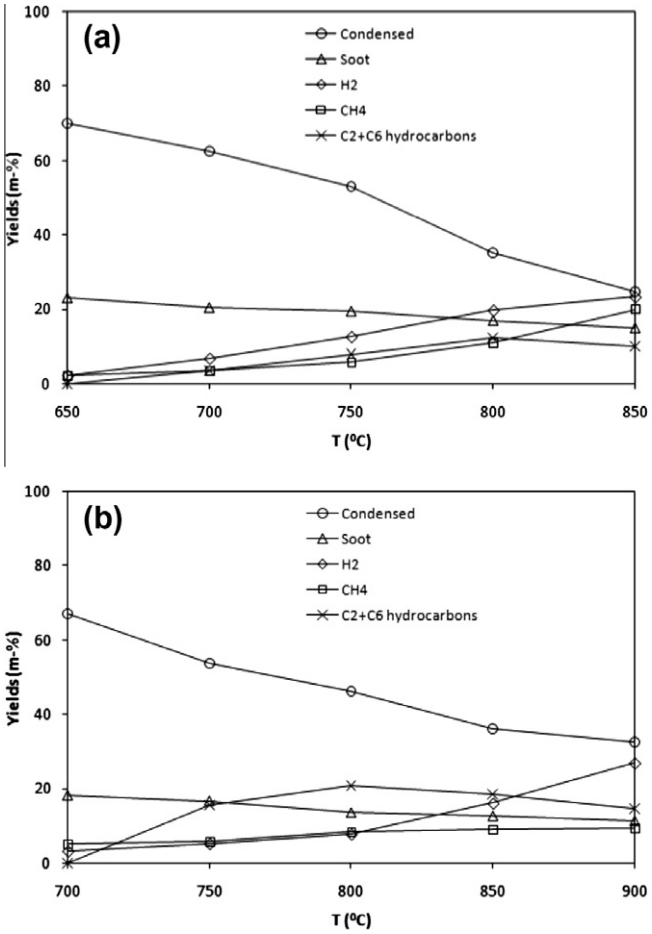

Fig. 5. Products yields during catalytic treatment of tar models using dolomite as a function of temperatures: (a) toluene and (b) naphthalene.

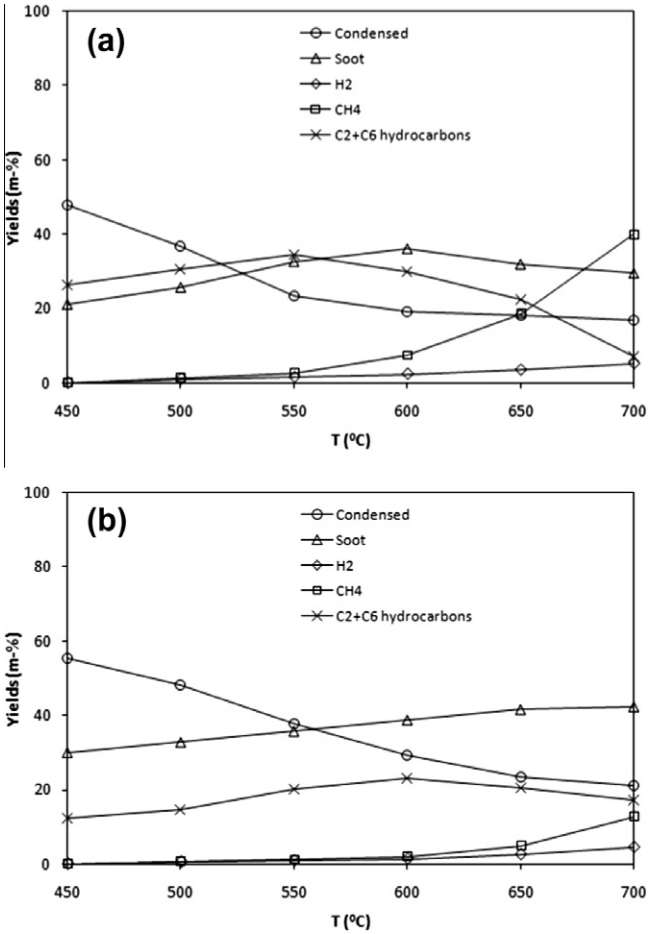

Fig. 6. Products yields during catalytic treatment of tar models using Y-zeolite as a function of temperatures: (a) toluene and (b) naphthalene.

dolomite, having higher pore size allows reaction of tar models on the surface, although its surface area is smaller than that of Y-zeolite.

The removal of toluene and naphthalene using Y-zeolite as a catalyst at various tested temperatures are shown in Fig. 6. Both toluene and naphthalene removal experiments were performed in the temperature range of 450–700 °C. The consideration of using relatively low temperature experiments with Y-zeolite as a catalyst in this study is based on the thermal stability of zeolites which varies from700 °C for low Si/Al ratios such as A-, X- and Y-zeolites to 1300 °C for high Si/Al ratios such as ZSM-5 (Gates, 1992). The results in Fig. 6(a) and (b) demonstrate that the removal of tar models increased significantly as the temperature increase to 550 °C for toluene and 650 °C for naphthalene. Further increase in temperature does not remove toluene and naphthalene significantly. The figure also evinced the different reactivity of toluene and naphthalene removal over Y-zeolite as a catalyst. Under the same operating condition (450–700 °C), toluene is easier to remove than naphthalene as also found in tar models removal with dolomite. At temperature of 750 °C, the lowest yields of condensed product of about 17% for toluene and 21% for naphthalene were obtained.

The decrease in condensed product with increase in temperature during toluene and naphthalene removal suggests the increasing role of cracking reaction and soot formation as shown in Eqs. (4)–(7). The large surface area, pore size and acidic nature of Y-zeolite also support cracking reaction and soot formation under condition investigated. As a result, the yield of gaseous products increases with temperature. CH_4 shows an exponential increase in its yield for both toluene and naphthalene removal. Moreover, at the highest temperature studied it became as the major product during catalytic treatment of toluene using Y-zeolite. Soot deposited onto the catalyst surface also increases with temperature especially for naphthalene removal whilst for toluene removal, the yield of soot start to decrease above 600 °C. At high temperature region, soot deposited mainly in the channels of catalyst, thereby lowering the surface area (Radwan et al., 2000). In addition, The TGA test results in general showed that the majority of soot formed on catalysts was heavy soot (high C content) that only can be burned at temperature above 550 °C. This is the reason for the insignificant removal of toluene and naphthalene at temperature above 550 °C and 650 °C, respectively. Another reason is due to the loss of catalytic surface area by thermal degradation which occurs at temperatures above 500 °C (Buchireddy et al., 2010).

The relatively high removal of toluene and naphthalene via both thermal and catalytic treatment in this study is not only caused by the long residence time, high temperature and catalysts activity but also due to increase of energy content of the tar molecules due to high intensity of electromagnetic radiation as mentioned also by Vreugdenhil and Zwart (2009). For instance, toluene as a model tar used in this study has ability to absorb electromagnetic energy with a loss tangent of 0.04 (Yin, 2012). The enhancement of reaction rates during RF irradiation has been broadly called the RF non-thermal effect. Compared to conventional heating, RF processing can increase the reaction rates of organic reactions about 10–1200 times (Gedye and Wei, 1998). In addition, although soot produced during thermocatalytic treatment of toluene and

naphthalene in this study can reduce the catalysts activity, however it also has a positive effect in RF processing which is able to absorb RF energy, resulting in the high frequency vibration of molecule and motion energy, and thus, self-heating.

4. Conclusions

A radio frequency tar treatment system which is low energy intensive, fast, and effective has been successfully developed for thermocatalytic treatment of tar model compounds. Temperature of 1200 °C can easily be obtained after 20 min of irradiation under power of 700 W, bed height of 120 mm and gas flow rate of 10 LPM. Thermal treatment processes of toluene and naphthalene become important at temperatures higher than 950 °C and 1100 °C, respectively. Soot appeared as the main product during thermal treatment of naphthalene. Soot free-gases were obtained with the use of catalysts. Y-zeolite has better catalytic activity compared to dolomite.

Acknowledgements

The authors gratefully acknowledge the E-ScienceFund awarded from Ministry of Science, Technology and Innovation (MOSTI) Malaysia along with RUI and PRGS Grant Universiti Sains Malaysia to carry out this work.

References

Anis, S., Zainal, Z.A., 2011. Tar reduction in biomass producer gas via mechanical, catalytic and thermal methods: a review. Renewable Sustainable Energy Rev. 15, 2355–2377.

Bergman, P.C.A., van Paasen, S.V.B., Boerrigter, H., 2003. The novel "OLGA" technology for complete tar removal from biomass producer gas. In: Bridgewater, A.V. (Ed.), Pyrolysis and Gasification of Biomass and Waste. CPL press, Newbury, pp. 347–356.

Boroson, M.L., Howard, J.B., Longwell, J.P., Peters, W.A., 1989. Heterogeneous cracking of wood pyrolysis tars over fresh wood char surfaces. Energy Fuels 3, 735–740.

Buchireddy, P.R., Bricka, R.M., Rodriguez, J., Holmes, W., 2010. Biomass gasification: catalytic removal of tars over zeolites and nickel supported zeolites. Energy Fuels 24, 2707–2715.

Bykov, Y.V., Rybakov, K.I., Semenov, V.E., 2001. High-temperature microwave processing of materials. J. Phys. D: Appl. Phys. 34, R55–R75.

Clark, D.E., Sutton, W.H., 1996. Microwave processing of materials. Annu. Rev. Mater. Sci. 26, 299–331.

Corella, J., Toledo, J.M., Padilla, R., 2004. Olivine or dolomite as in-bed additive in biomass gasification with air in a fluidized bed: which is better? Energy Fuels 18, 713–720.

Devi, L., Ptasinski, K.J., Janssen, F.J.J.G., van Paasen, S.V.B., Bergman, P.C.A., Kiel, J.H.A., 2005. Catalytic decomposition of biomass tars: use of dolomite and untreated olivine. Renewable Energy 30, 565–587.

Dou, B., Gao, J., Sha, X., Baek, S.W., 2003. Catalytic cracking of tar component from high-temperature fuel gas. Appl. Therm. Eng. 23, 2229–2239.

El-Rub, Z.A., 2008. Biomass Char as An In situ Catalyst for Tar Removal in Gasification Systems. Twente University, Enschede, The Netherlands.

Evans, R.J., Milne, T.A., 1997. Chemistry of tar formation and maturation in the thermochemical conversion of biomass. In: Bridgwater, A.V., Boocock, D.G.B. (Eds.), Developments in Thermochemical Biomass Conversion. Blackie Academic & Professional, London, pp. 803–816.

Fassinoua, W.F., Steeneb, L.V.D., Tourea, S., Volleb, G., Girard, P., 2009. Pyrolysis of Pinus pinaster in a two-stage gasifier: influence of processing parameters and thermal cracking of tar. Fuel Process. Technol. 90, 75–90.

Frenklach, M., Wang, H., 1994. Soot Formation in Combustion: Mechanisms and Models. In: Bockhorn, H. (Ed.). Springer-Verlag, Berlin, pp. 162–192.

Gates, B.C., 1992. Catalytic Chemistry. Wiley & Sons, Inc., Singapore.

Gedye, R.N., Wei, J.B., 1998. Rate enhancement of organic reactions by microwaves at atmosphere pressure. Can. J. Chem. 76, 525–532.

Gusta, E., Dalai, A.K., Uddin, M.A., Sasaoka, E., 2009. Catalytic decomposition of biomass tars with dolomites. Energy Fuels 23, 2264–2272.

Hofbauer, H., Fleck, T., Veronik, G., Rauch, R., Mackinger, H., Fercher, E., 1997. The FICFB-gasification process. In: Bridgwater, A.V., Boocock, D.G.B. (Eds.), Developments in Thermochemical Biomass Conversion. Blackie Academic & Professional, London, pp. 1016–1025.

Huang, Y.F., Kuan, W.H., Lo, S.L., Lin, C.F., 2010. Hydrogen-rich fuel gas from rice straw via microwave-induced pyrolysis. Bioresour. Technol. 101, 1968–1973.

Huang, Y.F., Kuan, W.H., Lo, S.L., Lin, C.F., 2008. Total recovery of resources and energy from rice straw using microwave-induced pyrolysis. Bioresour. Technol. 99, 8252–8258.

Jess, A., 1996. Mechanisms and kinetics of thermal reactions of aromatic hydrocarbons from pyrolysis of solid fuels. Fuel 75, 1441–1448.

Jones, D.A., Lelyveld, T.P., Mavrofidis, S.D., Kingman, S.W., Miles, N.J., 2002. Microwave heating applications in environmental engineering—a review. Resour. Conserv. Recycl. 34, 75–90.

Lee, B.-K., Jung, K.-R., Park, S.-H., 2008. Development and application of a novel swirl cyclone scrubber—(1) experimental. J. Aerosol Sci. 39, 1079–1088.

Milne, T.A., Evans, R.J., Abatzoglou, N., 1998. Biomass Gasifier "Tars": Their Nature, Formation, and Conversion. Report No. NREL/TP-570-25357NREL, Golden, CO, USA.

Namioka, T., Son, Y.-I., Sato, M., Yoshikawa, K., 2009. Practical method of gravimetric tar analysis that takes into account a thermal cracking reaction scheme. Energy Fuels 23, 6156–6162.

Radwan, A.M., Kyotani, T., Tomita, A., 2000. Characterization of coke deposited from cracking of benzene over USY zeolite catalyst. Appl. Catal., A 192, 43–50.

Salema, A.A., Ani, F.N., 2011. Microwave induced pyrolysis of oil palm biomass. Bioresour. Technol. 102, 3388–3395.

Simell, P.A., Hepola, J.O., Krause, A.O.I., 1997. Effects of gasification gas components on tar and ammonia decomposition over hot gas cleanup catalysts. Fuel 76, 1117–1127.

Sutton, W.H., 1989. Microwave processing of ceramic materials. Am. Ceram. Soc. Bull. 68, 376–386.

Sutton, W.H., 1992. Microwave processing of ceramics – an overview. In: Beatty, R.L., Sutton, W.H., Iskander, M.F. (Eds.), Microwave Processing of Materials III. Materials Research Society, pp. 3–20.

Tang, J., Hao, F., Lau, M., 2002. Microwave heating in food processing. In: Yang, X.H., Tang, J. (Eds.), Advances in Bioprocessing Engineering. World Scientific Publishing Co. Pte. Ltd., Singapore, pp. 1–44.

Thostenson, E.T., Chou, T.W., 1999. Microwave processing: fundamentals and applications. Composites Part A 30, 1055–1071.

Vreugdenhil, B.J., Zwart, R.W.R., 2009. Tar formation in pyrolysis and gasification. ECN-E-08-087.

Wicks, G.G., Clark, D.E., Schulz, R.L., 1998. Microwave technology for waste management applications including disposition of electronic circuitry. American Ceramic Society Annual Meeting.

Yin, C., 2012. Microwave-assisted pyrolysis of biomass for liquid biofuels production. Bioresour. Technol. 120, 273–284.

Zhang, Y., Kajitani, S., Ashizawa, M., Oki, Y., 2010. Tar destruction and coke formation during rapid pyrolysis and gasification of biomass in a drop-tube furnace. Fuel 89, 302–309.